DESIGN AND PERFORMANCE OF A COMPACT IMAGING SYSTEM FOR THE APS LINAC BUNCH COMPRESSOR *

B. X. Yang†, E. Rotela, N. Arnold, S. J. Stein, W. Berg, and S. Sharma
Advanced Photon Source, Argonne National Laboratory, Argonne, IL

Abstract

We present the design and performance of a high-resolution, high charge sensitivity imaging camera system for the APS linac beam profile measurement. Electron beam distribution is converted to light intensity distribution using standard YAG or optical transition radiation (OTR) screens. Two CCD cameras share the light through a beam splitter, each with its own imaging optics. One camera is normally set to a low magnification to give a full view of the converter screen (20 mm × 15 mm), and the other is set to a high magnification for measuring small beam. The overall dimension of the camera system is 400 mm × 165 mm × 110 mm. The focus and irises are driven by stepper motors and are remotely controlled. The fixed magnification and remotely controlled focus enable high reproducibility during beam-based setup of the optics. On bench test, the camera gave better then 10-μm resolution and better that 1% reproducibility of the magnification.

1 INTRODUCTION

A chicane bunch compressor was designed and implemented at the APS in 2000 [1] to increase the peak current of the bunch and improve the performance of the low-energy undulator test line (LEUTL) free-electron laser (FEL). It is expected to operate at ~200 MeV with normalized emittance in the range of 1 π to 4 π mm·mrad. Coherent synchrotron radiation (CSR) effects are expected to be significant at these emittance levels. Their study calls for accurate emittance measurement at the level of several percent or better.

Several authors [2-4] have shown that resolution at 10-micron level is well achievable for electron beam size measurements. The technical challenge here is to perform these measurements with the same high resolution, reliability, reproducibility, and accuracy needed. In this work, we describe a compact, modular imaging system designed to meet this challenge.

2 DESIGN SPECIFICATIONS

Table 1 shows the expected electron beam properties. In the bunch compressor region, the smallest beam size occurs in the region of three-screen measurements, where good accuracy is needed. Under the favorable conditions listed in Table 1, the error in the experimentally measured emittance $\Delta\varepsilon$ is related to the random error in the measured beam size $\Delta\sigma$ through the following relation, $\Delta\varepsilon/\varepsilon \approx \sqrt{2}\Delta\sigma/\sigma$, where σ is the measured beam size and ε is the derived emittance. Since the resolution of the camera is added to the measured beam size in quadrature, $\sigma_{\exp}^2=\sigma_{res}^2+\sigma^2$, the error due to optical resolution is given by, $\Delta\sigma = \left|\sqrt{\sigma^2+\sigma_{res}^2}-\sigma\right| \approx \sigma_{res}^2/2\sigma$. Therefore, the resolution-induced emittance error, if uncorrected, would be

$$\left(\frac{\Delta\varepsilon}{\varepsilon}\right) \approx \frac{1}{\sqrt{2}}\left(\frac{\sigma_{res}}{\sigma}\right)^2. \quad (1)$$

Table 1: Beam Parameters at the Three-Screen Section+

Electron energy (MeV)	200 (γ= 400)	
Single bunch charge (nC)	0.2 -- 1.0	
Normalized emittance (π mm·mrad)	4 .0	1.0
Emittance ε (π mm·mrad)	0.010	0.0025
Beta function at beam waist β (m)	1.00	
Dispersion: η (m)	0.00	
rms beam size, $\sqrt{\beta\varepsilon}$ (μm)	100	50

+ Three screens are equally spaced (1.0 meter) apart.

Uncertainties in beam size measurements come from many sources. We put them in five categories:

(1) Screen defect: non-homogeneity and imperfections of the converter screen, depth of source, saturation of scintillator, etc.
(2) Optics defect: imperfections of the mirrors, lenses, windows, etc.
(3) Resolution: optical resolution, defocus, camera pixel size, etc.
(4) Calibration: image distortion, calibration grid inaccuracy or distortion, operator error, etc.
(5) Statistics: finite counting statistics.

Many of these factors may be corrected by subtracting the resolution (more precisely, the rms width of the point spread function for the entire optical system) from the measured beam size. The true experimental error after the correction is normally a fraction of the "resolution," usually originating from properties that vary across the field of view or change over time. In this work, we take a conservative view that only 50% of the resolution effect is correctable. Table 2 shows the tolerance budget we give each source of errors / uncertainties.

The following actions were taken to bring the tolerance within budget:

(1) To reduce screen defect: We use well-polished thin scintillator crystals (0.1-mm-thick YAG) as converter screens, and implement a second, optical transition radiation (OTR) screen for use at high charge densities to avoid saturation.

* Work supported by U.S. Department of Energy, Office of Basic Energy Sciences, under Contract No. W-31-109-ENG-38.
† e-mail address: bxyang@aps.anl.gov

(2) To reduce optical defect: We use optical-quality vacuum windows and industrial- or research-grade (instead of consumer-grade) lenses and mirrors.

(3) Resolution: From Eq. (1) and Table 2, the resolution budget is 20% of the electron beam size, or 10 μm / 20 μm for beam emittance of 1 π / 4 π mm·mrad respectively. We maintain the cameras in focus by focusing remotely with the e-beam image.

(4) To improve calibration accuracy: We use a pinhole source mounted on translation stages and scan it in three dimensions. The calibration is maintained during installation and during refocus.

(5) To reduce statistical fluctuation: We maximize the entrance aperture of the optics. However, no in-vacuum lenses are used in order to avoid over-complication of the system at this point.

Table 2: Tolerance Budget for the Mini-Flag Cameras

	Size uncertainty	Emittance uncertainty
Screen defect	1.0 %	1.4 %
Optics defect	1.0 %	1.4 %
Resolution	2.0 %	2.8 %
Calibration	1.4 %	2.0 %
Statistics	2.0 %	2.8 %
TOTAL[+]	3.5 %	5 %

[+] Summations are in quadrature.

3 OPTICS DESIGN

While the camera is designed to accommodate lens systems for a wide range of magnifications, we present only one set of calculations here to demonstrate some of the information one obtains using ray tracing programs. Figure 1 shows the imaging optics we modeled with the ZEMAX ray tracing program.

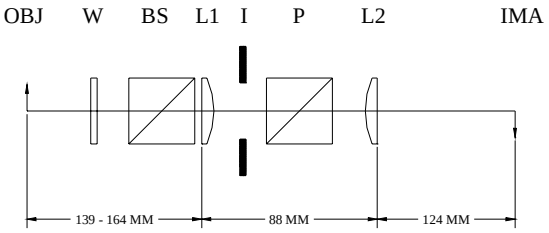

Figure 1: Geometry for ZEMAX ray tracing. The components are (OBJ) object; (W) vacuum quartz window; (BS) BK7 beam splitter; (L1) lens #1, a 150-mm FL achromat; (I) iris aperture; (P) 90º prism; (L2) lens #2, a 125-mm FL achromat; and (IMA) image plane.

Table 3 lists the rms radii of the point-spread function (PSF) for different configurations. Rows No. 4, 5, and 6 gives the resolution for cameras in focus, while rows No. 7 and 8 estimate the resolution when it is 200 μm out of focus. We can make the following observations: (1) for monochromatic light, the diffraction-limited resolution dominates at the focal plane; (2) for the narrow-band optics (corresponding to the spectrum of YAG scintillation) the resolution is dominated by the chromatic aberration; (3) for the broadband optics (corresponding to the OTR spectrum) the resolution further worsens by about a factor of two; and (4) when the object is 200 μm out of focus, the defocusing starts to dominate the total resolution. We conclude that the resolution for this design is within the budget given in Table 2, for both cases of 1 π and 4 π mm·mrad emittance.

Table 3 Rms Radii of the PSF Calculated with ZEMAX[+]

Configuration	Mono-chromatic	Narrow band	Broad-band
Wavelength (nm)	550	530±50	450-700
Diffraction peak	1.5 μm	1.5 μm	1.7 μm
Vacuum path alone	1.60 μm	5.2 μm	9.0 μm
+ 3.2 mm window	1.61 μm	5.4 μm	9.1 μm
+ Beam splitter & 90º prism	**1.8 μm**	**6.5 μm**	**10.3 μm**
Defocus +200 μm	10.1 μm	13.4 μm	15.1 μm
Defocus -200 μm	10.9 μm	10.4 μm	14.1 μm

[+] Radii include contribution from diffractions. Iris opening of 20 mm diameter was used in the calculation.

4 OPTO-MECHANICAL DESIGN

From the last two sections, the main goals of the opto-mechanical design are:

- Provide sturdy support for all optical components and two CCD cameras. Tolerance for lateral vibration is less than 5 μm.
- Make lens mounts available along the transport so that configurations of different magnification can be implemented as needed.
- Provide shielding for cameras from scattered ionizing radiation and from background light.
- Provide remote controlled motion for the entire optics / camera assembly, so that the focus can be maintained to within 200 μm and to keep the calibration unchanged.

The resulting design is shown in Figure 2. It is based on a 70-mm vacuum cube that can be mounted and operated in any orientation. We choose 25-mm achromat lens format for its availability in many focal lengths. Other design features of the flag system include:

(1) Two screens (YAG and OTR) are available at the same location.

(2) Two cameras, high-resolution and low-resolution (beam finder) cameras, are installed at the same location sharing the light through a beam splitter.

(3) A calibration grid is part of the camera to verify that bench calibrations have not changed in time.

(4) Focusing is remotely controlled to utilize two different types of screens and to maintain the camera in sharp focus.

(5) Irises are remotely controlled to operate the CCD at the appropriate intensity level.

(6) Two bends and tungsten enclosures are used to shield the CCD camera from line-of-sight paths to first (YAG screen) and most secondary scatterers. Only tertiary scattering can reach the camera. The

shielding thickness is 3.2 mm. To shield the camera from small-angle, high-energy shower, auxiliary shielding on the upstream side will be mounted.

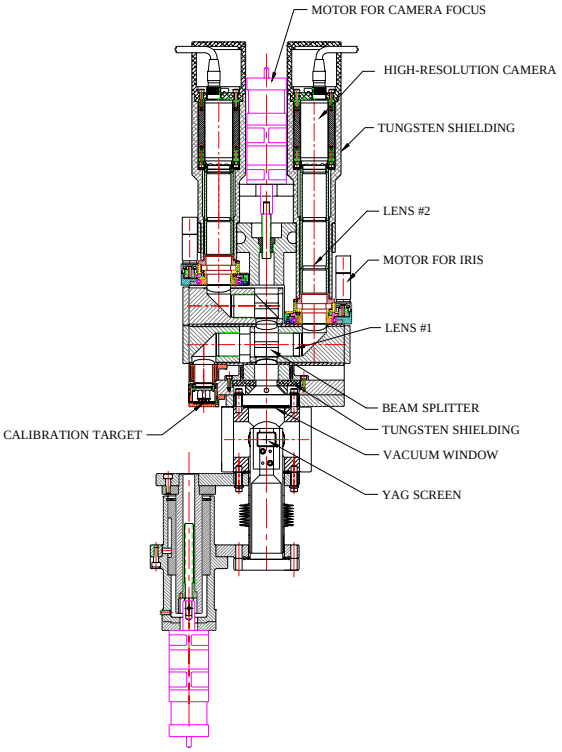

Figure 2: Schematic of the APS bunch compressor high-resolution camera.

5 CALIBRATION AND MEASUREMENT

In the past we have used machined features (straight edges, holes, etc.), as well as photographically-reduced dot-matrices / grids as calibration / focusing aids. But the results have not been very reproducible and sometimes even dependent upon the operator. These aids could not give us quantitative information about image properties that vary across the field of view. Additional errors are introduced when the dimensions of the grids vary from one station to another. In order to better characterize our cameras, we constructed a calibration stand, where the YAG screen is replaced with an illuminated 5-μm pinhole. The pinhole source is supported on precision translation stages, which scan in three dimensions with an accuracy of better than 5 μm over the entire travel. The video image of the pinhole is digitized, averaged, and fitted with Gaussian function [4]. With a UNIX script controlling the calibration processes, the pinhole is first positioned near the center of the video field and scanned longitudinally to locate the focal distance. Next, the source is put in focus but scanned in the transverse directions. Fitting the image centroid to the pinhole coordinate gives the calibration scale in μm/pixel. The raw data and the postprocessing graphs for every camera are stored as SDDS or postscript files and are accessible from that camera's control screens via HTML links.

The above procedures have been applied for a single camera multiple times to test for consistency. When the pinhole is adequately illuminated, the calibration results are reproducible to within 0.5%, well within budget (Table 2). The measured resolution for the configuration in Fig. 1 varies slightly from camera to camera, all between 8.5 and 9.5 μm.

Table 4 compares the measured beam size uncertainty with the design target. It is apparent that the camera assembly has achieved its original design goal. The cameras have been used for studies of the low-emittance beam [5]. While the initial results are encouraging, further characterization with electron beam is needed to better understand the effect of the converter screen, the interplay between the screen efficiency (counting statistics) and saturation, and to separate the linac's jitter from the statistical fluctuation.

Table 4: Beam Size Tolerances for the Mini-Flag Cameras ($\varepsilon = 1\ \pi$ mm·mrad)

	Achieved	Budget
Screen defect	To be studied	1 %
Optics defect & Resolution	1.8 %	2.2 %
Calibration	0.5 %	1.4 %
Statistics	2 % (?)†	2 %
TOTAL+	To be determined	3.5 %

+ Summations are in quadrature.

† It requires collection of >10 nC beam charge [5]. The actual beta function used was 0.6 m, reducing the beam size to 39 μm for beam with 1 π mm·mrad emittance.

6 ACKNOWLEDGEMENT

We wish to thank G. Decker, S. Milton, M. Borland, and A. Lumpkin for helpful discussions, encouragement, and support.

7 REFERENCES

[1] M. Borland et al., "A Highly Flexible Bunch Compressor for the APS LEUTL FEL," *Proc. LINAC 2000*, to be published.

[2] R. Autrata, et al., "Single-Crystal Aluminates - a New Generation of Scintillators for Scanning Electron Microscopes and Transparent Screens in Electron Optical Devices," *Scan. Elec. Micro.* 2, 489 (1983).

[3] W. S. Graves et al., "A High Resolution Electron Beam Profile Monitor and its Applications," AIP Proc. 451, 206 (1998).

[4] B. Yang et al, "Recent Developments in Measurement and Tracking of the APS Storage Ring Beam Emittance," *AIP Proc*. 546, 633 (2000).

[5] M. Borland et al., "Initial Characterization of Coherent Synchrotron Radiation Effects in the Advanced Photon Source Bunch Compressor," these proceedings.